

## THE VARIATIONS OF THE MAGNETIC Ap STAR 49 CAMELOPARDALIS

WALTER K. BONSAK, CATHERINE A. PILACHOWSKI, AND SIDNEY C. WOLFF

Institute for Astronomy, University of Hawaii

Received 1973 June 7

### ABSTRACT

The magnetic field of 49 Cam is found to vary cyclically between the limits of  $\pm 1.7$  kilogauss with a period of 4<sup>d</sup>285. Central depths of lines of Fe, Cr, and several rare earths are found to vary synchronously, with maximum strength corresponding to magnetic maximum. The photometric variation patterns are complex, with double minima occurring in the *b*- and *v*-bands of the four-color *uvby* system. The minima coincide with the magnetic extrema, and one minimum can be accounted for by variable line-blocking in the filter band. The results are discussed in terms of the rigid-rotator model.

*Subject headings:* magnetic stars — peculiar A Stars — spectrum variables — stars, individual

### I. INTRODUCTION

The peculiar nature of the spectrum of 49 Camelopardalis (HR 2977 = HD 62140) was first noted by Cowley (1968), who classified the star F0p, Sr-Eu, with the remark that the spectrum resembles  $\gamma$  Equ. The presence of a magnetic field in the star was established by van den Heuvel (1971) from measurements of the Zeeman effect in spectrograms obtained at the Lick Observatory. We began observations of 49 Cam at the Mauna Kea Observatory in 1971 in order to determine the details of the variation of the magnetic field, and the nature of any spectrum and light variations.

### II. OBSERVATIONS AND RESULTS

Spectrographic observations were made with the coudé spectrograph of the 224-cm telescope of the Mauna Kea Observatory, using the apparatus for observing the longitudinal Zeeman effect described by Wolff and Bonsack (1972). The spectrograms were obtained on baked Kodak IIA-O plates at a dispersion of  $6.8 \text{ \AA mm}^{-1}$ . The half-width of the instrumental profile is  $0.15 \text{ \AA}$ , approximately one-fourth the half-width of the observed stellar lines. The spectrograms were widened to 0.4 mm in each sense of circular polarization, and in most cases were suitable for spectrophotometry as well as wavelength measurement. Photometric calibration data were secured by means of an auxiliary calibration spectrograph.

The measurements and reduction of Zeeman shifts to obtain the effective longitudinal field,  $H_e$ , proceeded as described by Wolff and Bonsack (1972). The lines measured were chosen to sample various elements of interest, with predominant attention to the iron group. Blended lines were avoided, as were strong lines which would yield diminished Zeeman shifts because of saturation. The list consisted of 10 lines of Ti II, four lines of Cr I, two lines of Cr II, 15 lines of Fe I, four

lines of Fe II, three lines of Eu II, and two lines of Gd II—a total of 40 lines.

A smoothed direct-intensity microphotometer tracing was made for each spectrogram, separately for each sense of circular polarization. These tracings were inspected in detail for spectrum variation (no clear variation could be seen by visual inspection of the plates), and definite evidence for variable line depths and profiles was obtained. Subsequently, a set of lines was chosen for central-depth measurement on essentially the same criteria as given above, except that more rare-earth lines were included. The line list is given in table 1, which also gives the mean depth of each line, as a fraction of the continuum, averaged over all of the spectrograms. Plates of poor photometric quality were not measured for central depth.

The results of the *uvby* photometry suggested the importance of variations in the line-blocking coefficient in producing the light variation; consequently, we have measured the line-blocking coefficient for the *v*-band on six spectrograms selected for adequate coverage of the cycle. The measurement was made by direct numerical integration of digital microphotometer records, using as weights in the integration the product of the *v*-filter transmission (Crawford and Barnes 1970) and the continuum of an appropriate model atmosphere selected from the work of Mihalas (1966). Separate integrations were made for each sense of polarization on each of the six plates.

A summary of the numerical results from each spectrogram is given in table 2. Here column (1) gives the heliocentric Julian date of the middle of the exposure, and column (2) gives the corresponding phase according to the ephemeris given in § III. The next four columns give values of the magnetic field  $H_e$ : column (3) gives the field derived from the lines of titanium; column (4), the field from the lines of iron and chromium; column (5), the field from the lines of europium and gadolinium; and column (6), the mean

TABLE 1  
LINES MEASURED FOR VARIATION IN CENTRAL DEPTH

ID	$\lambda$ (Å)	Mean Central Depth	ID	$\lambda$ (Å)	Mean Central Depth
Fe I(695).....	4157.788	0.219	Ti II(41).....	4300.052	0.398
Fe I(597).....	4285.445	0.200	Ti II(41).....	4312.861	0.344
Fe I(68).....	4494.568	0.245	Ti II(40).....	4417.718	0.257
Fe II(22).....	4124.793	0.254	Eu II(5).....	3907.12	0.338
Fe II(32).....	4314.29	0.288	Eu II(1).....	4205.05	0.399
Fe II(37).....	4491.401	0.198	Eu II(4).....	4522.59	0.381
Cr I(23).....	3919.159	0.286	Gd II.....	4008.913	0.244
Cr I(1).....	4274.803	0.273	Gd II(15).....	4251.733	0.236
Cr I(287).....	4514.373	0.281	Ce II(4).....	4133.800	0.236
Cr II(19).....	4051.97	0.227	Ce II(10).....	4165.606	0.224
Cr II(182).....	4056.07	0.275	Nd II(25).....	3958.001	0.396
Cr II(31).....	4275.57	0.252			

field from all of the lines. Column (7) gives the radial velocity, reduced to the Sun, obtained from all of the lines. The relative line depths in columns (8) and (9) are the ratio of the depth of each line to the mean (table 1), averaged over both senses of polarization and over all lines of the group indicated. The last column gives the line-blocking coefficient for the photometric  $v$ -band.

The last row of table 2 gives a representative probable error for each column, computed as the mean of the individual internal probable errors. Entries in the table marked with a colon have internal probable errors which exceed the mean by more than 50 percent. The probable error for the line-blocking coefficient is the rms difference between the results for the two senses of polarization on each plate.

The results will be discussed in detail in § III, but we note at this point that the radial-velocity values do

not exhibit any significant variation with phase. The probable error of the result from a single plate, computed from the scatter in the plate means, is  $\pm 0.48$  km s<sup>-1</sup>, which agrees well with the mean internal probable error of  $\pm 0.41$  km s<sup>-1</sup>. The unweighted mean of the radial velocities is  $+7.20 \pm 0.12$  km s<sup>-1</sup>, which appears to differ significantly from the value of  $+1.9$  km s<sup>-1</sup> given by Wilson (1953), but is in better accord with the value of  $+5.3 \pm 0.3$  km s<sup>-1</sup> derived from van den Heuvel's (1971) results.

Four-color ( $uvby$ ) observations of 49 Cam were made with the 61-cm telescope of the Mauna Kea Observatory; the apparatus and techniques have been described by Wolff and Morrison (1973). The magnitudes and color indices derived for the two comparison stars are given in table 3, where the  $V$ -magnitudes have been derived from a linear transformation equation that relates  $y$  and  $V$  (Crawford and Barnes 1970).

TABLE 2  
SPECTROSCOPIC RESULTS

HJD (2,440,000+) (1)	PHASE (2)	$H_e$ (kilogauss)				$v_r$ km s <sup>-1</sup> (7)	RELATIVE LINE DEPTH		LINE-BLOCKING $v$ BAND (10)
		Ti II (3)	Fe + Cr (4)	Eu + Gd (5)	Mean (6)		Fe + Cr (8)	R.E. (9)	
1258.05.....	0.93	+1.37	+1.04	+1.08	+1.11	+7.7	...	...	...
1261.10.....	0.64	+1.91	+1.69	+0.96	+1.58	+6.8	1.17	1.25	0.33:
1268.10.....	0.27	-2.52	-1.03	-0.12	-1.10	+5.1	...	...	...
1270.00.....	0.72	+0.70	+1.40	+0.68	+1.12	+7.6	...	...	...
1271.05.....	0.96	-0.60	+0.48	-0.23	-0.22	+8.1	...	...	...
1272.02.....	0.19	-2.86	-1.62	-2.30	-1.99	+8.0	...	...	...
1297.01.....	0.02	-1.50	-0.38	-0.97	-0.72	+7.9	...	...	...
1325.11.....	0.58	+2.06	+2.34	+1.17	+2.04	+6.3	0.93	0.99	...
1326.00.....	0.78	+2.08	+1.25	+0.87	+1.36	+6.6	1.06	1.07	...
1398.83.....	0.78	+0.91:	+0.96	+0.54	+0.86	+5.1	1.11	1.10	0.31
1400.84.....	0.25	+0.18	-2.21	-2.53:	-1.74	+5.0	0.96	0.85	...
1432.82.....	0.71	+0.86	+0.64	-0.08	+0.53	+7.2	1.10	1.08	...
1433.80.....	0.94	+0.44	+0.73	-0.95:	+0.32	+6.8	0.98	0.97	...
1583.11.....	0.79	+1.87	+2.07	+1.82	+1.98	+7.9	0.98	1.00	0.28
1584.11.....	0.02	+0.71	-0.02	+0.35	+0.16	+9.0	0.92	0.96	0.27
1585.11.....	0.25	-0.61	-1.13	-0.12	-0.85	+8.0	0.90	0.81	0.26
1586.12.....	0.49	-0.36	+0.10	+1.72	+0.38	+8.3	0.89	0.92	0.27
Mean p.e.....		$\pm 0.42$	$\pm 0.26$	$\pm 0.59$	$\pm 0.21$	$\pm 0.4$	$\pm 0.10$	$\pm 0.08$	$\pm 0.01$

TABLE 3  
PHOTOMETRIC COMPARISON STARS

Star	$V$	$b - y$	$m_1$	$c_1$
HR 2946....	4.935	+0.048	+0.158	+1.157
HR 3106....	5.756	+0.266	+0.170	+0.501

The values are given to three decimal places in order to show precisely the differences in magnitude and color of the two stars. The results of the photometry of 49 Cam are given in table 4. The photometric results are plotted in figure 1 in terms of magnitudes in the individual bands, in order to give better insight into the nature of the variation.

### III. DISCUSSION

#### a) Periodic Variations

A search for a period to represent the variations of 49 Cam was carried out by applying a calculation based on the method of Lafler and Kinman (1965) to the magnetic field measurements. Of the periods suggested by this procedure, only one,  $4^d29$ , yielded a periodic variation in all quantities measured, with magnetic maximum coinciding with line-strength maxima in both the Fe-Cr and rare-earth line groups and with an extremum in the photometry. Such coincidence of the extrema of the variations is common among Ap stars (cf. Preston 1967*b*; Preston and Stępien 1968; and Wolff and Wolff 1971). The four measurements of  $H_e$  reported by van den Heuvel (1971) permitted us to improve the period further, leading to the ephemeris

$$\text{JD (negative crossover)} = 2,441,254.08 + 4.285E. \quad (1)$$

The epoch is the instant when  $H_e = 0$ ,  $dH_e/dt < 0$ , which is well defined by our data. The estimated uncertainty of the period is  $\pm 0^d001$ ; that of the epoch,  $\pm 0^d09$  (0.02 period).

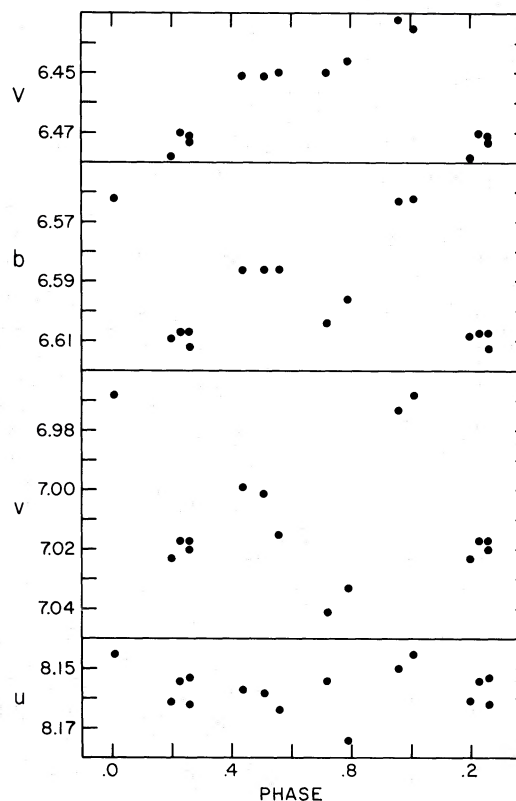


FIG. 1.—Four-color photometric variations of 49 Cam plotted according to the ephemeris JD (negative crossover =  $2,441,254.08 + 4.285E$ ). The probable error of a single point, excluding systematic zero-point effects, is  $\pm 0.003$  mag.

The results of the spectrographic measurements are plotted against phase in figure 2. A clear systematic variation is present in all cases, although for the magnetic field the scatter about the mean curve is rather more than would be predicted from the internal probable errors of the measurements. In the case of the line-depth variation, the curves are smoother than

TABLE 4  
PHOTOELECTRIC OBSERVATIONS

JD (2,440,000+)	Phase	$V$	$b - y$	$m_1$	$c_1$
1242.08.....	0.20	6.478	+0.130	+0.284	+0.720
1243.10.....	0.44	6.451	+0.135	+0.278	+0.745
1612.12.....	0.56	6.450	+0.137	+0.291	+0.721
1613.10.....	0.79	6.446	+0.151	+0.286	+0.706
1615.12.....	0.26	6.471	+0.141	+0.266	+0.734
1644.07.....	0.01	6.435	+0.127	+0.279	+0.771
1645.02.....	0.23	6.470	+0.136	+0.274	+0.727
1730.83.....	0.26	6.473	+0.134	+0.276	+0.726
1731.92.....	0.51	6.451	+0.135	+0.280	+0.742
1732.82.....	0.72	6.450	+0.154	+0.283	+0.676
1733.84.....	0.96	6.432	+0.131	+0.279	+0.767

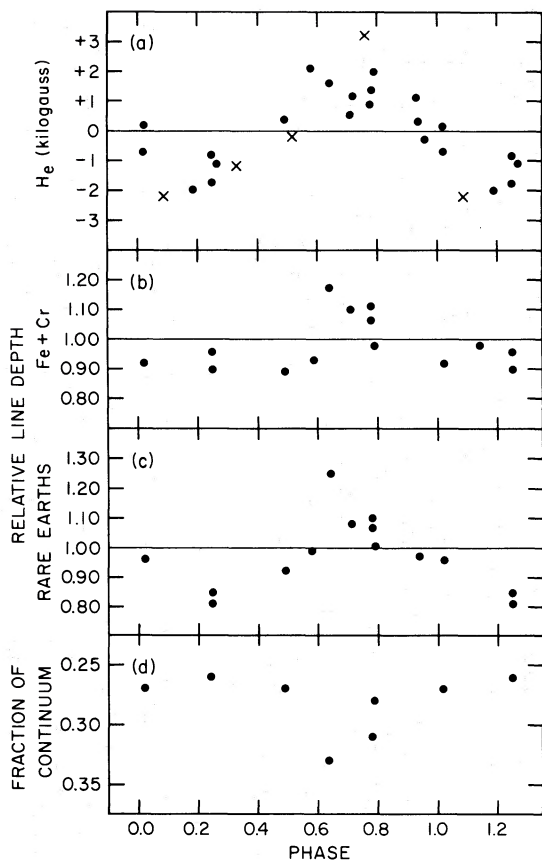


FIG. 2.—Spectroscopic variations of 49 Cam. (a) the variation in the magnetic field; (b) and (c) the variations in line depth for Fe + Cr and for the rare earths; (d) the variations in line-blocking in the  $v$  filter band. In the top panel, filled circles and crosses represent observations made at Mauna Kea and by van den Heuvel (1971), respectively. Probable errors for the plotted points are given in table 2.

one would expect: the scatter about the mean curves is less than predicted by the internal probable error of 8 percent. However, the internal errors are inflated by averaging over lines of different strengths, which would be expected to respond differently to any physical cause of the variation, and over the two senses of polarization.

The  $v$  and  $b$  light curves in figure 1 exhibit a remarkable double wave character, which we believe to be real for several reasons. First, the depths of the minima exceed by at least a factor of 8 the typical probable error (0.003 mag) of a single observation (Wolff and Wolff 1971; Wolff and Morrison 1973). Second, the shape of the light curve indicated by observations on four consecutive nights in 1973 February is exactly the same as is obtained by phasing together the remaining photometric observations by means of the period derived from the magnetic data. Third, the minima in the light curve coincide in phase

with extrema in the curves that show the variations of magnetic intensity and line strengths.

Wolff and Wolff (1971) have suggested that coincident line and light maxima may be caused by a back-warming effect due to very strong line blanketing in the ultraviolet—a suggestion which was recently confirmed by Molnar (1973) for  $\alpha^2$  CVn from OAO data. In cooler stars, with less flux in the ultraviolet and more lines in the filter bands, local blanketing may be expected to compete with the back-warming effect. The  $v$ -band line-blocking shown in the lower panel of figure 2 exhibits an increase of 7 percent of the continuum at phase 0.8, which accounts quantitatively for the dip of 0.07 mag at that phase in the  $v$  photometry shown in figure 1. The reduction of the strength of this minimum in the  $b$ - and  $y$ -bands is to be expected from reduced density of absorption lines in these bands; our spectrographic data do not permit calculation of the line-blocking for these bands.

The light minimum at phase 0.2 is interpreted as representing the nearest approach to the unblanketed flux. As the line strength increases toward phase 0.8, the flux is first increased by back warming due to line blanketing in the ultraviolet; but this effect is overwhelmed except in the  $y$ -band by local line-blocking. The difference between 49 Cam and  $\alpha^2$  CVn in this regard is presumably due to the temperature. The mean  $b - y$  color of 49 Cam is +0.14, which, using the correlation with  $B - V$  given by Crawford and Barnes (1970) and the temperature scale of Morton and Adams (1968), corresponds to a temperature of 8200° K and a spectral type of A7 V. The temperature of  $\alpha^2$  CVn is near 10,000° K (Molnar 1973). The reduction of the range of the light variation in the  $u$ -band is similar to that found by Molnar in  $\alpha^2$  CVn.

#### b) Differences between Elements

In her study of the magnetic field of HD 188041, Wolff (1969) found that the amplitude of the magnetic field depended on the element which was observed, and interpreted the result as indicating a different distribution over the stellar surface of the various elements considered. We have searched for a similar effect in 49 Cam by forming differences between the magnetic field measured in the lines of Fe and Cr and in the lines of the other two groups of elements, in the sense  $\Delta H(X) = H_e(\text{Fe, Cr}) - H_e(X)$ . The probable error of the difference was formed from the individual internal probable errors, and the weighted average  $\langle \Delta H(X) \rangle$  was computed for all of the spectrograms, with the reciprocals of the squares of the probable errors used as weights. The results were

$$\langle \Delta H(\text{Ti II}) \rangle = +0.12 \pm 0.12 \text{ kilogauss,}$$

$$\langle \Delta H(\text{Eu, Gd}) \rangle = +0.38 \pm 0.12 \text{ kilogauss.}$$

The latter value appears to be significantly different from zero.

As Wolff has pointed out, systematic differences may arise from errors in the effective Zeeman splittings,  $z$ , which are computed from  $LS$  coupling theory, which is a poor approximation for rare-earth spectra. Errors may also arise from saturation effects if there is a systematic difference in the strengths of the lines in the two groups. However, both these errors affect the magnitude of the field and not the sign, and should tend to cancel when averaged over a symmetrically reversing magnetic cycle. For our data, we would expect such cancellation to be incomplete, because most of the spectrograms were taken during the positive half of the cycle. To test this possibility, means of  $\Delta H(\text{Eu}, \text{Gd})$  were computed for the two halves of the cycle separately, and the two values were insignificantly different from each other and from the mean given above.

We conclude that the magnetic field indicated by the lines of Eu II and Gd II is systematically more negative at all phases by about 400 gauss than the field obtained from lines of Cr and Fe.

#### c) *Nonperiodic Variations*

As mentioned above, the scatter of individual data points about the curves representing the magnetic variations in figure 2 is larger than would be expected on the basis of the internal probable errors. Substantial scatter in magnetic-field data is not rare; and in the case of 78 Vir, Preston (1969*b*) concluded that the scatter could be accounted for by systematic effects which differed from plate to plate, particularly with regard to the alignment of the plate on the measuring machine.

All but two of the spectrograms of 49 Cam were measured by Bonsack, and several were measured more than once. Pilachowski measured the two additional plates, as well as repeating the measurement of one other. In all cases where measurements were repeated, the results agreed to within the accuracy predicted by the internal probable errors. We conclude that deviations of individual points from the mean curve of up to five probable errors are probably intrinsic in the behavior of the star, and not artifacts of the measurement. Unfortunately, there are not enough data to distinguish between cycle-to-cycle systematic differences and random fluctuations. Further investigation of short-term or nonrepetitive effects seems warranted, not only in 49 Cam but in other Ap stars as well.

#### d) *Rotation*

The projected equatorial rotational velocity of 49 Cam,  $v \sin i$ , was estimated by comparing the tracings of the spectrum with those of a low-rotation comparison star, after convolving the latter with broadening functions for various degrees of rotation. This technique is similar to that employed by Danziger and Faber (1972). Our low-rotation comparison star was

$\gamma$  Equ, which has a spectrum generally similar to 49 Cam, and a value of  $v \sin i$  less than  $3 \text{ km s}^{-1}$  (Evans and Elste 1971). A tracing covering the range  $\lambda\lambda 4200\text{--}4400$  was made of a spectrogram of  $\gamma$  Equ with a dispersion of  $3.4 \text{ \AA mm}^{-1}$ , widened to 0.8 mm in one sense of circular polarization. The digital record of this tracing was smoothed and broadened with a function to reduce the resolution to that of the  $6.8 \text{ \AA mm}^{-1}$  spectrograms used for 49 Cam. The resulting record was then broadened successively by a series of rotational broadening functions for various values of  $v \sin i$ , and the results plotted on the same scale as the tracings of 49 Cam. The rotational broadening function was that given by Unsöld (1955); the limb-darkening coefficient was obtained by interpolating in the limb-darkening data given by Danziger and Faber with the temperature of  $7700^\circ \text{ K}$  given for  $\gamma$  Equ by Evans and Elste. The choice of limb-darkening coefficient proved to have little effect on the resulting line profiles.

The best match between the tracings of 49 Cam and the broadened tracings of  $\gamma$  Equ was found for  $v \sin i = 22 \text{ km s}^{-1}$ , with an estimated uncertainty of  $\pm 3 \text{ km s}^{-1}$ . The matching process included attention to both the line profiles and the resolution of close pairs of lines.

Following Preston (1972), we estimate the equatorial velocity from the period using the formula  $v = 137/P$   $\text{km s}^{-1}$ , which assumes a radius of  $2.7 R_\odot$  for a late A-type star. With the period of  $4^d 285$ , this formula gives  $v = 32.0 \text{ km s}^{-1}$  for 49 Cam. Combined with the above estimate of  $v \sin i$ , we obtain the angle  $i = 43^\circ \pm 7^\circ$  between the line of sight and the axis of rotation.

#### IV. SUMMARY: A MODEL

The principal features of the variations of 49 Cam can be summarized in terms of a rigid-rotator model. The period of  $4^d 285$  is taken as the period of rotation, which, when combined with the measured projected equatorial velocity,  $v \sin i$ , of  $22 \text{ km s}^{-1}$  and an estimate of the radius, yields an angle of  $43^\circ$  between the line of sight and the axis of rotation.

The symmetrically reversing nature of the curve of magnetic field variation indicates that the field can be represented by a dipole lying close to the plane of the rotational equator (cf. Preston 1967*a*). Thus, at the extremes of the magnetic cycle, the angle between the line of sight and the field axis is approximately  $47^\circ$ . Following Preston (1969*a*), we find that the measured effective field of 2 kilogauss implies a dipole field of strength 10 kilogauss at the magnetic pole. The measurements of  $H_e$  plotted in figure 2 suggest that the cycle may be slightly asymmetric, with the field positive approximately 55 percent of the time. This implies that the angle between the pole of the axis of rotation nearest the observer and the positive magnetic pole is slightly less than  $90^\circ$ , in which case the effective

field should be stronger at positive extremum than at the negative. The scatter in the data is sufficient to mask a small difference of this nature.

The variations in line strength and light are explained by a slight concentration of the metal and rare-earth abundances into the hemisphere of the positive magnetic field. The abundance variation directly produces the observed line variation, and the double-wave light variation is caused by a combination of line blanketing in the filter band and in the unobserved ultraviolet. The concentration of the elements to the magnetic pole is not sufficiently sharp to produce moving cores in the rotationally broadened line profiles, or line doubling, which would lead to measurable variations in radial velocity.

The concentration of the rare-earth abundance to the positive magnetic pole, as indicated by the line strength variations, appears to contradict the observation that the field indicated by the lines of Eu II and Gd II is systematically more negative than the field indicated by Fe and Cr. Such an effect might result if the rare-earth atoms are less concentrated to the positive pole than the iron-group atoms, and if in the negative hemisphere, where all abundances are some-

what lower, the rare earths are more concentrated to the pole.

In summary, the rigid-rotator model provides a basis for understanding the systematic variations of 49 Cam, which is one of the more rapidly varying of the known magnetic Ap stars. The location of the magnetic poles near the rotational equator is the configuration most frequently found in previously studied cases (Preston 1967*a*). Of unique interest is our success in ascribing one of the features of the photometric variation to line-blocking in the filter band. Superposed upon this rotating configuration is a mechanism which produces fluctuations in the magnetic field. Our data are insufficient to indicate the characteristics of this mechanism, but the problem is clearly worthy of further study.

This research was supported by National Science Foundation grant GP-29741. During the latter stages of the work, Bonsack was a Visiting Astronomer at the Kitt Peak National Observatory, and gratefully acknowledges the hospitality extended by Director L. Goldberg and Associate Director A. A. Hoag.

#### REFERENCES

- Cowley, A. 1968, *Pub. A.S.P.*, **80**, 453.  
 Crawford, D. L., and Barnes, J. V. 1970, *A.J.*, **75**, 978.  
 Danziger, I. J., and Faber, S. M. 1972, *Astr. and Ap.*, **18**, 428.  
 Evans, J. C., and Elste, G. 1971, *Astr. and Ap.*, **12**, 428.  
 Heuvel, E. P. J. van den. 1971, *Astr. and Ap.*, **11**, 461.  
 Laffer, J., and Kinman, T. D. 1965, *Ap. J. Suppl.*, **11**, 216.  
 Mihalas, D. 1966, *Ap. J. Suppl.*, **13**, 1.  
 Molnar, M. R. 1973, *Ap. J.*, **179**, 527.  
 Morton, D. C., and Adams, T. F. 1968, *Ap. J.*, **151**, 611.  
 Preston, G. W. 1967*a*, *Ap. J.*, **150**, 547.  
 ———. 1967*b*, *ibid.*, p. 871.  
 ———. 1969*a*, *ibid.*, **156**, 967.  
 Preston, G. W. 1969*b*, *Ap. J.*, **158**, 243.  
 ———. 1972, *ibid.*, **175**, 465.  
 Preston, G. W., and Stepien, K. 1968, *Ap. J.*, **151**, 583.  
 Unsöld, A. 1955, *Physik der Sternatmosphären* (2d ed.; Berlin: Springer-Verlag), p. 508.  
 Wilson, R. E. 1953, *General Catalogue of Stellar Radial Velocities* (Washington: Carnegie Institution of Washington).  
 Wolff, S. C. 1969, *Ap. J.*, **157**, 253.  
 Wolff, S. C., and Bonsack, W. K. 1972, *Ap. J.*, **176**, 425.  
 Wolff, S. C., and Morrison, N. D. 1973, *Pub. A.S.P.*, **85**, 141.  
 Wolff, S. C., and Wolff, R. J. 1971, *A.J.*, **76**, 422.